Ring surface waves in thermal nonlinear media

Yaroslav V. Kartashov,[1] Victor A. Vysloukh,[2] and Lluis Torner[1]

[1]*ICFO-Institut de Ciencies Fotoniques, and Universitat Politecnica de Catalunya, Mediterranean Technology Park, 08860 Castelldefels (Barcelona), Spain*

[2]*Departamento de Fisica y Matematicas, Universidad de las Americas – Puebla, Santa Catarina Martir, 72820, Puebla, Mexico*

Yaroslav.Kartashov@icfo.es

Abstract: We address ring-shaped surface waves supported by defocusing thermal media with circular cross-section. Such waves exist because of the balance between repulsion from the interface and deflection of light from the bulk medium due to defocusing nonlocal nonlinearity. The properties of such surface waves are determined by the geometry of the sample. Nodeless ring surface waves are stable for all values of their winding number, while surface waves with a small number of azimuthal nodes can be metastable.

© 2007 Optical Society of America

OCIS codes: (190.0190) Nonlinear optics; (190.6135) Spatial solitons

References and links

1. W. Krolikowski, O. Bang, N. I. Nikolov, D. Neshev, J. Wyller, J. J. Rasmussen, and D. Edmundson, "Modulational instability, solitons and beam propagation in spatially nonlocal nonlinear media," J. Opt. B: Quantum and Semiclass. Opt. **6**, S288 (2004).
2. C. Conti, M. Peccianti, and G. Assanto, "Observation of optical spatial solitons in highly nonlocal medium," Phys. Rev. Lett. **92**, 113902 (2004).
3. M. Peccianti, C. Conti, and G. Assanto, "Interplay between nonlocality and nonlinearity in nematic liquid crystals," Opt. Lett. **30**, 415 (2005).
4. M. Peccianti, C. Conti, G. Assanto, A. De Luca, and C. Umeton, "Routing of anisotropic spatial solitons and modulational instability in liquid crystals," Nature **432**, 733 (2004).
5. M. Peccianti, A. Dyadyusha, M. Kaczmarek, and G. Assanto, "Tunable refraction and reflection of self-confined light beams," Nature Physics **2**, 737 (2006).
6. C. Rotschild, O. Cohen, O. Manela, M. Segev, and T. Carmon, "Solitons in nonlinear media with an infinite range of nonlocality: first observation of coherent elliptic solitons and of vortex-ring solitons," Phys. Rev. Lett. **95**, 213904 (2005).
7. C. Rotschild, B. Alfassi, O. Cohen, and M. Segev, "Long-range interactions between optical solitons," Nat. Phys. **2**, 769 (2006).
8. C. Rotschild, M. Segev, Z. Xu, Y. V. Kartashov, L. Torner, and O. Cohen, "Two-dimensional multipole solitons in nonlocal nonlinear media," Opt. Lett. **31**, 3312 (2006).
9. D. Briedis, D. Petersen, D. Edmundson, W. Krolikowski, and O. Bang, "Ring vortex solitons in nonlocal nonlinear media," Opt. Express **13**, 435 (2005).
10. A. I. Yakimenko, Y. A. Zaliznyak, and Y. Kivshar, "Stable vortex solitons in nonlocal self-focusing nonlinear media," Phys. Rev. E **71**, 065603(R).
11. A. M. Deykoon and G. A. Swartzlander, "Pinched optical-vortex soliton," J. Opt. Soc. Am. B **18**, 804 (2001).
12. S. Lopez-Aguayo, A. S. Desyatnikov, Y. S. Kivshar, S. Skupin, W. Krolikowski, and O. Bang, "Stable rotating dipole solitons in nonlocal optical media," Opt. Lett. **31**, 1100 (2006).
13. Y. V. Kartashov, L. Torner, V. A. Vysloukh, and D. Mihalache, "Multipole vector solitons in nonlocal nonlinear media," Opt. Lett. **31**, 1483 (2006).
14. B. Alfassi, C. Rotschild, O. Manela, M. Segev, and D. N. Christodoulides, "Boundary force effects exerted on solitons in highly nonlocal nonlinear media," Opt. Lett. **32**, 154 (2007).
15. A. Minovich, D. Neshev, A. Dreischuh, W. Krolikowski, and Y. Kivshar, "Experimental reconstruction of nonlocal response of thermal nonlinear optical media," Opt. Lett. **32**, 1599 (2007).
16. N. N. Akhmediev, V. I. Korneyev, and Y. V. Kuzmenko, "Excitation of nonlinear surface-waves by Gaussian light-beams," Zh. Eksp. Teor. Fiz. **88**, 107 (1985).
17. *Nonlinear waves in solid state physics*, Ed. by A. D. Boardman, M. Bertolotti, and T. Twardowski, NATO ASI **247**, Plenum Press, New York (1989).
18. D. Mihalache, M. Bertolotti, and C. Sibilia, "Nonlinear wave propagation in planar structures," Prog. Opt. **27**, 229 (1989).

19. A. D. Boardman, P. Egan, F. Lederer, U. Langbein, and D. Mihalache, "Third-order nonlinear electromagnetic TE and TM guided waves," in *Nonlinear Surface Electromagnetic Phenomena*, Ed. by H. E. Ponath and G. I. Stegeman (North Holland, Amsterdam, 1991), 73-287.
20. P. Varatharajah, A. Aceves, J. V. Moloney, D. R. Heatley, and E. M. Wright, "Stationary nonlinear surface waves and their stability in diffusive Kerr media," Opt. Lett. **13**, 690 (1988).
21. D. R. Andersen, "Surface-wave excitation at the interface between diffusive Kerr-like nonlinear and linear media," Phys. Rev. A **37**, 189 (1988).
22. Y. V. Kartashov, L. Torner, and V. A. Vysloukh, "Lattice-supported surface solitons in nonlocal nonlinear media," Opt. Lett. **31**, 2595 (2006).
23. B. Alfassi, C. Rotschild, O. Manela, M. Segev, and D. N. Christodoulides, "Nonlocal surface-wave solitons," Phys. Rev. Lett. **98**, 213901 (2007).
24. Y. V. Kartashov, F. Ye, V. A. Vysloukh, and L. Torner, "Surface waves in defocusing thermal media," Opt. Lett. **32**, 2260 (2007).

Nonlocality is an intrinsic feature of many optical materials [1]. Among the strongly nonlocal materials which can be used for the experimental exploration of soliton formation are liquid crystals [2-5] and thermal media [6-8]. Besides the simplest solitons, such materials support several types of stable, higher-order two-dimensional structures [9-13].

Light beams propagating in nonlocal media cause refractive index changes in regions far exceeding the beam width, therefore the beam trajectory can be strongly altered by the presence of interfaces, like in thermal media where the induced refractive index profile is determined by the sample geometry [14,15]. Under proper conditions light may concentrate in the vicinity of the interface, exciting surface waves in both local [16-19] and nonlocal nonlinear materials [20-24]. Two-dimensional surface waves at the interface of focusing thermal medium were observed in Ref [23]. Also, thermal materials with defocusing nonlinearity have been shown to support one-dimensional surface waves [24].

In this paper we reveal that thermal samples of circular cross-section with a defocusing nonlinearity support specific ring-profile surface waves localized near the outer edge of the sample. Such waves form due to the balance between repulsion from the interface and deflection of light from the bulk sample due to a defocusing nonlinearity.

We consider the propagation of laser beam along the ξ axis of a defocusing thermal medium with circular cross-section, described by the equations for the field amplitude q and nonlinear contribution to the refractive index n :

$$i\frac{\partial q}{\partial \xi} = -\frac{1}{2}\left(\frac{\partial^2 q}{\partial r^2} + \frac{1}{r}\frac{\partial q}{\partial r} + \frac{1}{r^2}\frac{\partial^2 q}{\partial \phi^2}\right) - qn,$$

$$\frac{\partial^2 n}{\partial r^2} + \frac{1}{r}\frac{\partial n}{\partial r} + \frac{1}{r^2}\frac{\partial^2 n}{\partial \phi^2} = |q|^2.$$

(1)

Here the radial and longitudinal coordinates r, ξ are scaled to the beam radius and the diffraction length, respectively; ϕ is the azimuthal angle. Equation (1) was solved with the boundary conditions $q, n|_{r \to R} = 0$ (R is the sample radius; here we set $R = 20$, but results remain valid for other radiuses), corresponding to the situation when light does not penetrate into the regions outside the thermal sample, whose surface is maintained at a fixed temperature. Physically, this can be achieved when the refractive index of the surrounding material, that plays the role of heat sink, is much lower than that of the thermal medium. In this case the beam propagating in the cylindrical rod experiences slight absorption, that causes an increase and a redistribution of temperature in the entire medium due to heat diffusion.

We assume a typical situation where the refractive index decreases in the heated regions. Such a decrease causes light defocusing and thus expulsion of light from the bulk material toward its periphery. In circular samples the repulsion from the interface with the less opti-

cally dense surrounding medium results in light localization in the vicinity of interface in the form of bright rings that may feature azimuthal or angular nodes.

Radially symmetric surface waves can be found in the form $q(r, \phi, \xi) = w(r) \exp(im\phi) \times \exp(ib\xi)$, where m is the topological charge, and b is the propagation constant. For such excitations the refractive index is given by

$$n(r, \xi) = \int_0^R G_0(r, \rho) |q(\rho, \xi)|^2 \, d\rho, \tag{2}$$

where $G_0(r, \rho) = \rho \ln(\rho / R)$ for $r < \rho$ and $G_0(r, \rho) = \rho \ln(r / R)$ for $r \geq \rho$ is the response function of the medium. For the linear stability analysis we will looking at solutions in the form $q = [w(r) + u(r, \xi) \exp(ik\phi) + v^*(r, \xi) \exp(-ik\phi)] \exp(ib\xi + im\phi)$, where the perturbations components u, v can grow with a complex rate $\delta = \delta_r + i\delta_i$ upon propagation, and k is the azimuthal perturbation index. Substitution into Eq. (1) and linearization yields the eigenvalue problem

$$i\delta u = -\frac{1}{2} \left[\frac{d^2 u}{dr^2} + \frac{1}{r} \frac{du}{dr} - \frac{(m+k)^2}{r^2} u \right] - w\Delta n_k - un + bu,$$
$$i\delta v = \frac{1}{2} \left[\frac{d^2 v}{dr^2} + \frac{1}{r} \frac{dv}{dr} - \frac{(m-k)^2}{r^2} v \right] + w\Delta n_k + vn - bv, \tag{3}$$

where

$$\Delta n_k = \int_0^R G_k(r, \rho) w(\rho) [u(\rho) + v(\rho)] d\rho \tag{4}$$

is the refractive index perturbation corresponding to the azimuthal index k, while $G_k(r, \rho) = -(\rho / 2k)[(r / \rho)^k - (r\rho / R^2)^k]$ for $r < \rho$, and $G_k(r, \rho) = -(\rho / 2k)[(\rho / r)^k - (r\rho / R^2)^k]$ for $r \geq \rho$.

Nodeless ring-shaped surface waves exist for $b \leq 0$ [as depicted in Fig. 1(a)]. With decreasing b, the peak amplitude of the surfaces waves increases, while the separation between the interface and the wave peak intensity decreases. A decrease in b is accompanied by a monotonic growth of the energy flow [as seen in Fig. 1(d)]

$$U = 2\pi \int_0^R rw^2 dr \tag{5}$$

and by an enhanced localization of light near the sample boundary. The degree of localization may be measured by the radial width of the surface wave, which is found to be a monotonically increasing function of b [Fig. 1(e)]. Despite the fact that light is localized near the sample edge, the refractive index exhibits a flat plateau across most of the sample [see Fig. 1(b)], and it is locally increased in the vicinity of the sample edge. Such increase gives rise to surface waves. The decrease in the refractive index in the center of the sample becomes more pronounced with increasing light intensity.

We also found solutions with various number n_r of radial nodal lines [Fig. 1(c)]. For such waves the local intensity maximum located farthest from the edge is always the most pronounced. Despite the presence of radial oscillations in w, the refractive index always has a shape similar to those shown in Fig. 1(b). At fixed b, the energy flow carried by the wave with larger n_r is smaller [Fig. 1(d)]. Ring surface waves with any n_r can carry screw phase

dislocations characterized by a winding number, or topological charge, m. Since rings are localized near the outer sample edge and their radii are close to R, the profiles of waves with moderate m values are almost identical.

Surface wave localization is achieved due to the balance set between the expulsion from the bulk of the defocusing sample and the repulsion from its edge. Note that in this setting, any potential azimuthal instabilities are suppressed and all nodeless waves are stable for any m. The instability suppression occurs because in defocusing media a local increase of the
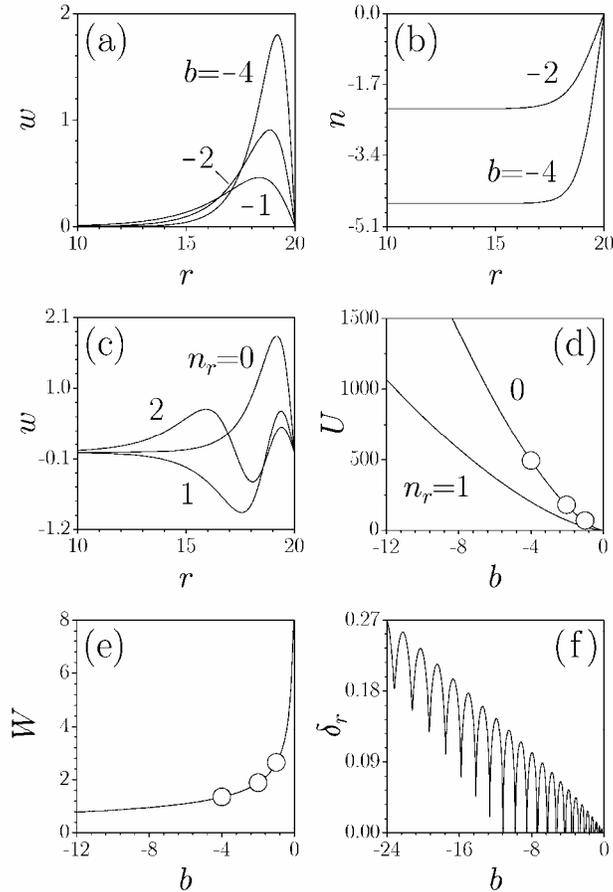

Fig. 1. Profiles (a) and refractive index distributions (b) for nodeless surface waves with $m = 0$, $n_r = 0$ for different b values. (c) Profiles of surface waves with different n_r at $b = -4$, $m = 0$. (d) Energy flow versus b for surface waves with different n_r at $m = 0$. (e) Integral width of surface wave with $n_r = 0$, $m = 0$ versus b. Points marked by circles in (d) and (e) correspond to waves shown in (a). (f) Real part of perturbation growth rate corresponding to $k = 1$ for wave with $m = 0$, $n_r = 1$ versus b.

light intensity at a given spatial point caused by the azimuthal modulation results in a decrease of the refractive index in the vicinity of this point. Therefore, light tends to deflect from such regions, thus restoring an azimuthally uniform distribution. At the same time, deflection from the bulk sample and repulsion from its edge ensure that light remains radially localized near the sample edge. In our comprehensive numerical experiments, nodeless waves keep their

structure for huge distances in the presence of the strong random and regular perturbations (Fig. 2, top). Note that in all cases shown in Figs. 2 and 3, weak multiplicative azimuthal perturbations $[1 + 0.002\sum_{p=1}^{N}\cos(p\phi)]$ with $N \gg 1$ were added to the stationary field distribu-
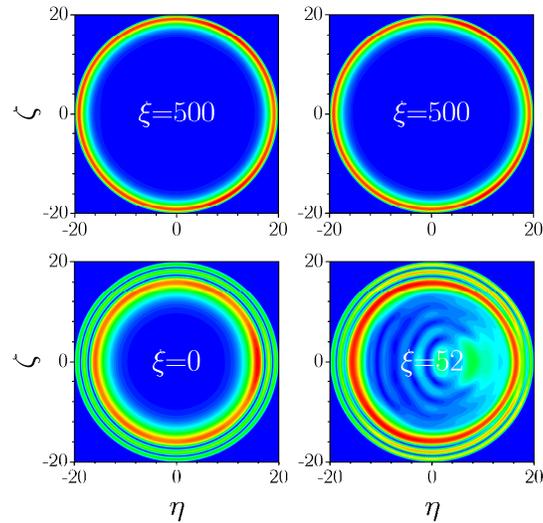

Fig. 2. Propagation of perturbed surface waves with different n_r. Field modulus distributions for waves with $n_r = 0$, $m = 0$ (top, left), $n_r = 0$, $m = 3$ (top, right), $n_r = 2$, $m = 0$ (bottom) are shown at different distances. All waves correspond to $b = -4$.
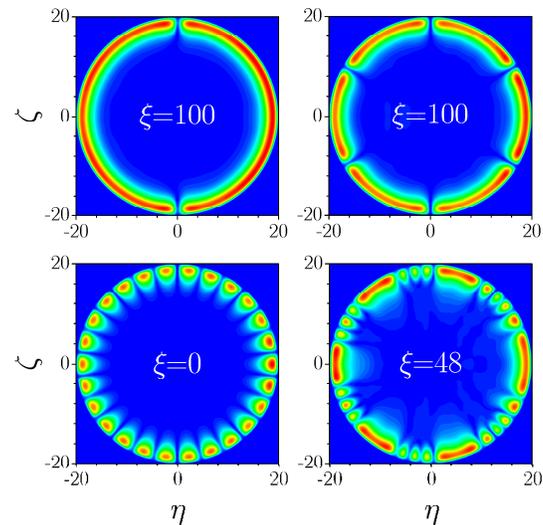

Fig. 3. Propagation of perturbed surface waves with different n_ϕ. Field modulus distributions for waves with $n_\phi = 2$ (top, left), $n_\phi = 6$ (top, right), and $n_\phi = 26$ (bottom) are shown at different distances. All waves correspond to $b = -2$.

tions with the aim to trigger any potential azimuthal instabilities. Thus, the input in Fig. 2 that would be radially symmetric without perturbation appears slightly distorted. All higher-order waves with $n_r > 0$ are turn out to be oscillatory unstable. Figure 1(f) shows the dependence

of the perturbation growth rate δ_r on b for the wave with $n_r = 1$. For a fixed azimuthal index k there are regions (close to $b = 0$) where δ_r vanishes, but they overlap with regions where δ_r is nonzero for other values of k. The decay of waves with radial nodes is accompanied by the gradual fusion of their rings (Fig. 2, bottom) that occurs faster at higher energy flows.

We also found surface waves with azimuthal nodal lines, featuring necklace-like shapes with phase changing by π between the bright spots forming such waves. Representative profiles, obtained from Eq. (1) in the form $q(r, \phi, \xi) = w(r, \phi) \exp(ib\xi)$, are shown in Fig. 3. The energy flow of such waves increases with decreasing b, while the radial width decreases. The higher the number of nodal lines n_ϕ the smaller the energy flow at fixed b. Far from the azimuthal nodes, such waves resemble the previously discussed rings, especially for small values of n_ϕ (see the top panel in Fig. 3). The refractive index profile exhibits a plateau in the center of the sample, but close to the sample edge it is azimuthally modulated.

Rigorously speaking, all surface waves with $n_\phi > 0$ were found to be unstable. This was confirmed by comprehensive simulations in the presence of regular and noisy perturbations for different b and n_ϕ values. In all cases, in our numerical simulations azimuthally modulated solutions self-destroyed after propagation over sufficiently large distances. However, the corresponding perturbation growth rates may be extraordinarily small for waves with small n_ϕ values and at moderate energy flows. The decay distances for such waves, when they are strongly perturbed, far exceeds the experimentally available sample lengths (see the top row of Fig. 3 showing a long-distance propagation of perturbed waves with $n_\phi = 2$ and 6). As expected on intuitive grounds, increasing the number of azimuthal nodes substantially enhances instabilities at fixed b. Waves with large n_ϕ quickly decay via increasing oscillations of bright spots (as illustrated in the bottom panel of Fig. 3). However, waves with small n_ϕ should be readily observed experimentally in short sample lengths.

Summarizing, we have found that the balance between expulsion from the bulk of defocusing thermal media and repulsion from their edge may result in the formation of new types of surface waves, that exhibit ring-like shapes in accordance with the sample geometry.

Acknowledgements